Exploring Multi-shot non-CPMG for Hyperpolarized 13C Metabolic MR Spectroscopic Imaging

Y-F. Yen[1], P. Le Roux[2], D. Mayer[3,4], A. Takahashi[1], J. Tropp[1], D. Spielman[3], A. Pfefferbaum[4,5], and R. Hurd[1]
[1]Global Applied Science Laboratory, GE Healthcare, Menlo Park, CA, United States, [2]Global Applied Science Laboratory, GE Healthcare, France, [3]Radiology, Stanford University, Stanford, CA, United States, [4]Neuroscience Program, SRI International, Menlo Park, CA, United States, [5]Psychiatry and Behavioral Sciences, Stanford University, Stanford, CA, United States

Introduction

We developed a new MR spectroscopic imaging (MRSI) sequence that utilizes non-CPMG[1,2] echo trains with quadratic phase modulation of the refocusing pulses to catalyze the stability of longitudinal magnetization while keeping the transverse magnetization refocused during the echo train. Other alternative phase modulation schemes (such as XY, MLEV) are useful only over a very restricted range, close to π, of the refocusing pulse rotation angle (nutation)[1]. The non-CPMG phase scheme with realignment[3] performs well for nutations as low as 160° and, with a proper design of RF pulses for a wide spectral bandwidth, this technique is suitable for fast spectroscopic imaging. Because non-CPMG allows us to obtain a full magnitude signal even in the presence of initial phase variation, we can perform multiple low flip-angle excitations with echo-train readouts without waiting for the longitudinal signal to recover via T_1 relaxation, a condition ideal for spectroscopic imaging of hyperpolarized nuclei. In this report, we show preliminary test results of Multi-Excitation Non-CPMG with LOw flip angles (MENLO) sequence and two of its potential applications: 2D T_2 mapping and 3D MRSI. The tests were performed on ^{13}C-enriched phantoms as well as animals with hyperpolarized [1-^{13}C]pyruvate injections.

Method

***Pulse Sequence*:** The sequence consists of a slice-selective excitation pulse and a non-selective non-CPMG echo train. EPI trajectories were used to acquire spin-echo signals for 2D spatial encoding. Chemical-shift encoding was accomplished by shifting TE from excitation to excitation. Therefore, the amount of TE shift is inversely proportional to the spectral bandwidth and the number of spectral points determines the number of excitations. The echo spacing depends on the desired X and Y spatial resolutions as well as the spectral resolution. For 2D T_2 mapping, EPI acquisition was repeated from echo to echo in order to collect signals undergoing T_2 decay. For 3D-MRSI, the third spatial dimension was encoded with phase-encoding gradients during the echo train. Isotropic 5mm resolution was obtained for all experiments in this report, but better resolution can be achieved if signal to noise ratio permits. All experiments were conducted on a 3T Signa™ MR Scanner (GE Healthcare, Waukesha, WI, USA) using a dual-tuned 1H/13C quadrature coil[4].

Phantom Experiment: The off-resonance performance was tested on a 2-cm diameter spherical phantom containing 2M of ^{13}C-acetate by varying the center frequency from –500 to +500Hz off-resonance. The stability of longitudinal magnetization was tested on 80mM hyperpolarized [1-^{13}C]pyruvate solution (hyp-^{13}C-pyr) collected in a syringe, with a constant 5.6° flip-angle excitation every 3 seconds (TR) for 4 minutes. A non-CPMG echo train of 32 echoes was used and all encoding gradients were turned off (MENLO dynamics). The data were compared with a pulse-and-acquire measurement of the same flip angles and TR. MENLO T_2 mapping was validated on both the ^{13}C-acetate phantom and hyp-^{13}C-pyr phantom, and the T_2 values were compared to the T_2 measured by a single-voxel CPMG sequence[5]. The image quality of MENLO 3D-MRSI were evaluated on a hyp-^{13}C-pyr phantom in comparison with 3D-EPSI data acquired in the same scan time (results not shown here).

***Animal Experiment*:** Four healthy Wistar rats (178 to 433 g) were used to test the MENLO sequence for 2D T_2 mapping and 3D-MRSI of rat head. Respiration, rectal temperature, heart rate, and oxygen saturation were monitored throughout the experiment. The animal was kept warm by using a water blanket regulated at 37ºC. Animal preparation and physiological monitoring followed a protocol approved by the Stanford University Institutional Animal Care and Use Committee.

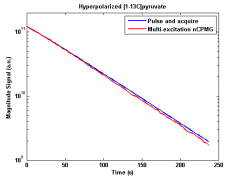

Fig. 1: MENLO dynamics (red) in good agreement with pulse-and-acquire (blue) of hyp-^{13}C-pyr.

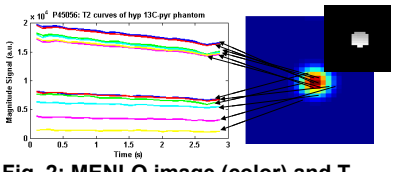

Fig. 2: MENLO image (color) and T_2 curves (plot) of a hyp-^{13}C-pyr phantom. Voxel-by-voxel curve fitting yielded a T_2 map (gray-scale insert) with T2 = 15 ± 2s.

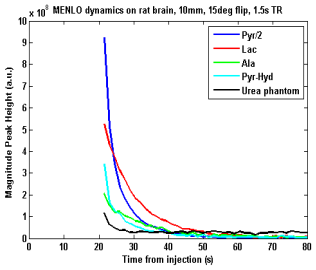

Fig. 3: MENLO dynamics of a 10mm axial slice on a rat head.

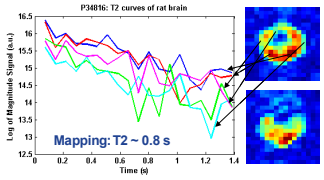

Fig. 4: MENLO images (right) and T_2 curves (log plot) of a rat head following a hyp-^{13}C-pyr injection. The two images were extracted from two spectral peaks, which yet to be identified.

Results

Consistent MENLO performance was obtained within a 780Hz off-resonance bandwidth (not shown). In phantoms, longitudinal magnetization was well stabilized as demonstrated by the close agreement between MENLO dynamics and pulse-and-acquired data over 80 excitations (Fig.1). Good image quality was obtained in the T_2 mapping of acetate (not shown) and hyp-^{13}C-pyr phantoms (Fig.2). The ^{13}C-acetate T_2 values (2.8 ± 0.3s) from MENLO were smaller than the T_2 (4.7s) obtained from the single-voxel CPMG T_2 measurement. MENLO dynamics of a rat head showed fast signal loss in pyruvate but the lactate signal persisted slightly longer (Fig. 3). The MENLO images of a rat head from 2D T_2 mapping (Fig.4) were extracted from two spectral peaks but their identifications are yet to be determined. T_2 curves of consistent quality are shown in Fig.4 and the average T_2 of rat head is 0.8s. For comparisons, the single-voxel (whole brain) CPMG T_2 measurement of the same rat yielded T_2 of 0.6s for pyruvate and 1.1s for lactate. For *in vivo* MENLO 3D-MRSI, one of the 8 slices of pyruvate is shown in Fig. 5, which has similar image quality as the 3D-EPSI of pyruvate.

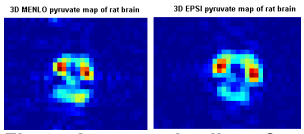

Fig. 5: An example slice of MENLO 3D-MRSI of pyruvate (left) compared to the same slice by 3D-EPSI (right).

Discussion and Conclusion

MENLO works well in phantoms, though there is some degradation *in vivo*, probably due to blood flow. Flowing spins that experience different B1 within the coil and sharp B1 changes at the edges of the coil are more difficult to refocus. This would be less of a problem when using a large whole-body transmit coil. Improvements are being made to tackle these problems, as well as T_2 quantitation. Better chemical-shift encoding strategies are being tested to improve *in vivo* spectral quality.

Acknowledgments NIH grants RR09784, AA05965, AA13521-INIA, and EB009070.

Reference

1) P. Le Roux. J Magn Reson 2002; 155:278. 2) M. Bastin and P. Le Roux. Magn Reson Med 2002; 48:6. 3) P. Le Roux and Y.F. Yen. MAGMA vol 22, Suppl 1, abstract 114, 2009. 4) K. Derby, et al. J Magn Reson 1990; 86:645. 5) Y-F. Yen, et al. Proc. of the 17th Annual Meeting of ISMRM, Honolulu, USA, 2009. p 4377.